

PERCEPTUAL QUALITY ASSESSMENT FOR DIGITAL HUMAN HEADS

Zicheng Zhang, Yingjie Zhou, Wei Sun, Xiongkuo Min, and Guangtao Zhai

Institute of Image Communication and Network Engineering, Shanghai Jiao Tong University, China
zzc1998@sjtu.edu.cn

ABSTRACT

Digital humans are attracting more and more research interest during the last decade, the generation, representation, rendering, and animation of which have been put into large amounts of effort. However, the quality assessment for digital humans has fallen behind. Therefore, to tackle the challenge of digital human quality assessment issues, we propose the first large-scale quality assessment database for scanned digital human heads (DHHs). The constructed database consists of 55 reference DHHs and 1,540 distorted DHHs along with the subjective ratings. Then, a simple yet effective full-reference (FR) projection-based method is proposed. The pretrained Swin Transformer tiny is employed for hierarchical feature extraction and the multi-head attention module is utilized for feature fusion. The experimental results reveal that the proposed method exhibits state-of-the-art performance among the mainstream FR metrics. The database and the method presented in this work will be made publicly available.

Index Terms— Digital human head, quality assessment database, full-reference, projection-based

1. INTRODUCTION

Digital humans are digital simulations and models of human beings on computers [1], which have been widely employed in applications such as games, medicine industry, automobiles, etc. Current research scopes are mainly focused on the generation, representation, rendering, and animation of digital humans [2]. However, with the rapid development of VR/AR environments, more and more viewers demands digital human perception with higher visual quality in real-time manners, which makes it necessary to carry out objective models for digital human quality assessment (DHQA). Unfortunately, the collection of digital human models is very expensive and time-consuming, which requires the assistance of professional three-dimensional (3D) scanning devices and human subjects. Moreover, large-scale subjective experiments on the visual quality of digital humans are not available currently. Therefore, it is meaningful to carry out a quality assessment database targeted at digital humans.

In this paper, we propose a large-scale quality assessment database for digital human heads (DHHs). A total of

255 human subjects are invited to participate in the DHH scanning experiment. We carefully select 55 generated high-quality DHH models as the reference stimuli (the DHH models are in the format of textured meshes), which covers both male and female, young and old. Then we manually degrade the reference DHHs with 7 types of distortions (surface simplification, position compression, UV compression, texture sub-sampling, texture compression, color noise, and geometry noise) and obtain 1,540 distorted DHHs in total. Afterwards, a well-controlled subjective experiment is conducted to collect mean opinion scores (MOS) for the distorted DHHs. Consequently, we successfully carry out the largest subject-rate quality assessment database for digital human heads (DHHQA). On the DHHQA database, we validate several mainstream quality assessment metrics for the benchmark. Further, we specifically design a deep neural network (DNN) based full-reference (FR) quality assessment method to boost the performance. The experimental results show that the proposed method has a better correlation with the subjective ratings and achieves better performance than other quality assessment metrics.

2. RELATED WORKS

2.1. Digital Human

Sensing, Modeling, and driving digital humans have been popular research topics in computer vision and computer graphics. During the last decade, large amounts of work have been carried out to deal with the digital human related issues. Namely, digital human action recognition [8, 9] aims to understand digital human motion activities. 3D human pose and shape estimation [10, 11] of great significance for the representation of digital human models. Digital human reconstruction [12, 13] is targeted at reconstructing digital human models from key points or 2D media. However, little attention is paid to the visual quality assessment of digital humans.

2.2. 3D Quality Assessment

Currently, 3D quality assessment (3D-QA) mainly focuses on point cloud quality assessment (PCQA) and mesh quality assessment (MQA). To cope with the challenge of visual quality

Table 1. The comparison of 3D-QA databases and our database.

Database	Source	Subject-rated Models	Content	Description
SJTU-PCQA [3]	10	420	Colored Point Cloud	Humans, Statues
WPC [4]	20	740	Colored Point Cloud	Fruit, Vegetables, Tools
LSPCQA [5]	104	1,240	Colored Point Cloud	Animals, Humans, Vehicles, Daily objects
CMDM [6]	5	80	Colored Mesh	Humans, Animals, Statues
TMQA [7]	55	3,000	Textured Mesh	Statues, Animals, Daily objects
DHHQA(Ours)	55	1,540	Textured Mesh	Scanned Real Human Heads

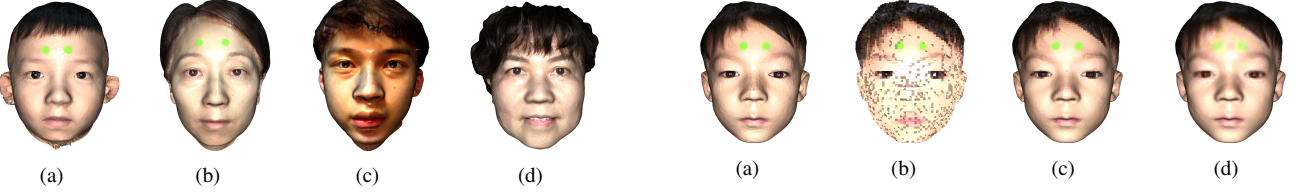


Fig. 1. DHH samples from the DHHQA database.

assessment of 3D models, substantial efforts have been made to carry out 3D quality assessment databases [3, 4, 5, 6, 7] and the detailed comparison with the proposed database is listed in Table 1, from which we can find that the proposed DHHQA database is the first large-scale database specially designed for DHHs.

The objective quality assessment methods for 3D-QA can be generally categorized into two types: model-based methods [6, 4, 5, 14] and projection-based methods [3, 15, 7]. Model-based methods extract features directly from 3D models while projection-based methods infer the visual quality of 3D models from the rendered projections. Although the model-based methods are invariant to viewpoints, it is difficult to efficiently extract quality-aware features from 3D models since the high-quality 3D models usually contain large numbers of dense points/vertices. While the projection-based methods can make use of the mature image/video quality assessment (IQA/VQA) models, therefore gaining higher practical value.

3. DATABASE CONSTRUCTION

3.1. DHH Collection & Distortion Generation

To gather the source models of DHHs, we invite 255 human subjects (aged from 12 to 60) to participate in the scanning experiment with the Bellus3D [16] app. Finally, a total of 55 DHHs are manually chosen as the source DHH models. Samples of the selected DHHs are exhibited in Fig. 1. Then 7 types of common distortions are applied to degrade the reference DHH models: (a) Surface simplification: The algorithm proposed in [17] is employed to simplify the DHH models and the simplification rate is set as {0.4, 0.2, 0.1, 0.05}; (b) Position Compression: The Draco [18] library is applied to

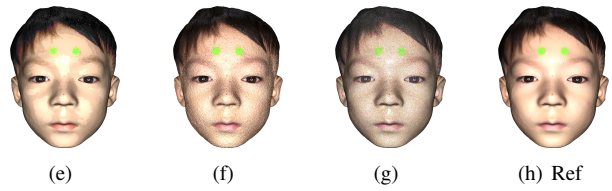


Fig. 2. Examples of DHH models with different types of distortions, where the sub-figure index are of the same order as the distortion description in section 3.1.

quantize the position attributes of the DHH models with compression parameter qp set as {6, 7, 8, 9}; (c) UV Map Compression: The Draco library is applied to quantize the texture coordinate attributes with the compression parameter qt set as {7, 8, 9, 10}; (d) Texture Down-sampling: The reference texture maps (4096×4096) are down-sampled with resolutions of $\{2048 \times 2048, 1024 \times 1024, 512 \times 512, 256 \times 256\}$; (d) Texture Compression: The JPEG compression is used to compress the texture maps with quality levels set as {3, 10, 15, 20}; (e) Geometry Noise: Gaussian noise is introduced to the vertices of the DHH models with σ_g set as {0.05, 0.1, 0.15, 0.2}; (f) Color Noise: Gaussian noise is added to the texture maps with σ_c set as {20, 40, 60, 80}. To sum up, $1,540 = 55 \times 7 \times 4$ distorted DHH models are generated and the degradation levels are manually defined to cover the most quality range.

3.2. Subjective Experiment

Following the recommendation of ITU-R BT.500-13 [19], we conduct the subjective experiment in a well-controlled laboratory environment. All the DHH models are rendered into projections from the front and left side viewpoint and the reference as well as distorted projections are at the same time for evaluation. The projections are shown in random order with

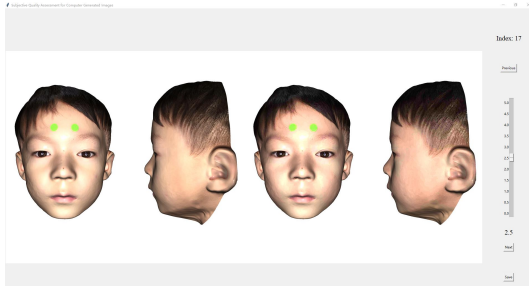


Fig. 3. Illustration of the rating interface.

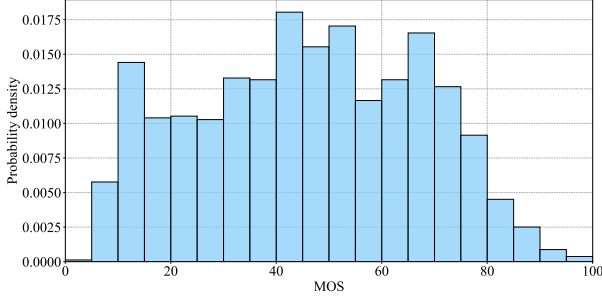


Fig. 4. Distribution of the MOSs.

an interface designed by Python Tkinter on an iMac monitor which supports the resolution up to 4096×2304 , the screenshot of which is illustrated in Fig. 3. 22 males and 18 females are invited to participate in the subjective experiment. The whole experiment is divided into 11 sessions. Each session contains 140 distorted DHH models and is attended by at least 20 participants. In all, more than $30,800 = 1,540 \times 20$ subjective ratings are collected.

After the subjective experiment, we calculate the z-scores from the raw ratings as follows:

$$z_{ij} = \frac{r_{ij} - \mu_i}{\sigma_i}, \quad (1)$$

where $\mu_i = \frac{1}{N_i} \sum_{j=1}^{N_i} r_{ij}$, $\sigma_i = \sqrt{\frac{1}{N_i-1} \sum_{j=1}^{N_i} (r_{ij} - \mu_i)^2}$, and N_i is the number of images judged by subject i . The ratings from unreliable subjects according to ITU-R BT.500-13 [19]. The corresponding z-scores are linearly rescaled to $[0, 100]$ and the mean opinion scores (MOSs) are computed by averaging the rescaled z-scores. The MOS distribution is exhibited in Fig. 4, from which we can see that the quality ratings cover most of the quality range.

4. OBJECTIVE QUALITY ASSESSMENT

To provide useful guidelines for quality-oriented digital human systems, we propose a simple yet effective full-reference (FR) projection-based method to predict the visual quality of DHH models. The framework of the proposed method is il-

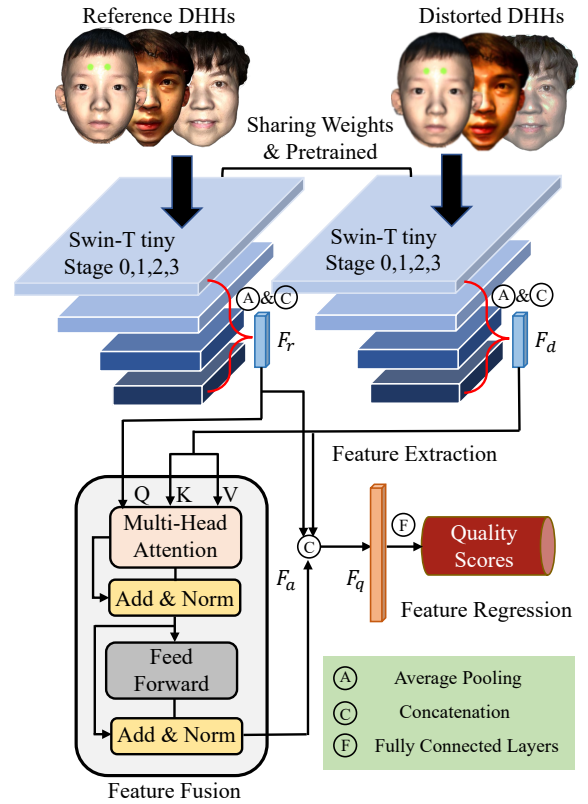


Fig. 5. Framework of the proposed method.

lustrated in Fig. 5, which includes the feature extraction, the feature fusion module, and the feature regression module.

4.1. Feature Extraction

To ensure the efficiency and effectiveness, the pretrained Swin Transformer tiny (ST-t) [20] is employed as the feature extraction backbone. To further make use of the multi-scale features that are essential for quality assessment tasks, we employ the hierarchical structure for feature extraction:

$$\begin{aligned} En(x) &= \alpha_0(x) \oplus \alpha_1(x) \oplus \alpha_2(x) \oplus \alpha_3(x), \\ \alpha_k(x) &= AP(S_k(x)), k \in \{0, 1, 2, 3\}, \end{aligned} \quad (2)$$

where $S_k(x)$ represents the features from the k -th stage, $AP(\cdot)$ stands for the average pooling operation, $\alpha_k(x)$ denotes the pooled results from the k -th stage and \oplus indicates the concatenation operation. Given the input reference and distorted front projections P_r and P_d , the quality-aware features can be obtained as:

$$F_r = En(P_r), F_d = En(P_d), \quad (3)$$

where $En(\cdot)$ is the hierarchical ST-t encoder, F_r and F_d represent the quality-aware embeddings for the input reference and distorted front projections.

4.2. Feature Fusion

To actively relate the quality-aware information between the reference and distorted embeddings, we utilize the multi-head attention operation for feature fusion:

$$\begin{aligned} F_a &= \Gamma(Q = F_r, K = F_d, V = F_d), \\ F_q &= F_r \oplus F_d \oplus F_a, \end{aligned} \quad (4)$$

where $\Gamma(\cdot)$ indicates the multi-head attention operation where F_r is used to guide the attention learning of F_d , F_a is the fused quality-aware embedding, and F_q is the final quality embedding.

4.3. Feature Regression

With the final quality embedding F_q , two stage fully-connected (FC) layers are employed for feature regression:

$$Q' = FC(F_q), \quad (5)$$

where Q' represents the predicted quality scores and $FC(\cdot)$ stands for the fully-connected layers. Moreover, the L1 loss is utilized as the loss function:

$$Loss = \frac{1}{n} \sum_{\eta=1}^n |Q_\eta - Q'_\eta|, \quad (6)$$

where n is the size of the mini-batch, Q_η and Q'_η are quality labels and predicted quality scores respectively.

5. EXPERIMENT

5.1. Implementation Details & Competitors

The ST-t backbone is fixed with weights pretrained on the ImageNet [21] and only the feature fusion and regression module are trained. The Adam optimizer [22] is used with the initial learning rate set as 1e-4 and the number of training epochs is set as 50. The batch size is set as 32. The 1080×1920 front projections are resized into the resolution of 256×456 and patches with the resolution of 224×224 as the input. We conduct the 5-fold cross validation on the DHHQA database and the average results of the 5 folds are recorded as the final performance. It's worth mentioning that there is no content overlap between the training and testing sets. Several mainstream FR-IQA methods are validated for comparison as well, which includes PSNR, SSIM [23], MS-SSIM [24], GMSD [25], VIF [26], and LPIPS [27]. These methods are validated using the same front projections on the same testing sets as the proposed method and the average results are recorded as the final performance. Additionally, all the quality scores predicted by the IQA methods are processed with five-parameter logistic regression to deal with the scale difference.

Table 2. Performance comparison on the DHHQA database. Best in bold.

Model	SRCC	PLCC	KRCC	RMSE
PSNR	0.8347	0.8371	0.6405	11.5822
SSIM	0.7355	0.7253	0.5388	14.5221
MS-SSIM	0.8557	0.8396	0.6653	11.4953
GMSD	0.8411	0.8350	0.6534	11.6441
VIF	0.8898	0.8885	0.7058	9.7018
LPIPS	0.7199	0.7416	0.5309	14.2062
Proposed	0.9286	0.9320	0.7585	7.2910

5.2. Performance Discussion

The performance results are shown in Table 1, from which we can several inspections: (a) The proposed method achieves the higher performance among all the competitors and is about 0.03 ahead of the second place competitor VIF (0.9286 vs. 0.8898) in terms of SRCC, which shows the effectiveness of the proposed method for predicting the visual quality of DHH models; (b) Most IQA methods obtain relatively good performance on the DHHQA database with SRCC values higher than 0.8 except SSIM and LPIPS; (c) Comparing the performance of MS-SSIM and SSIM, we can conclude that the multi-scale features can greatly help boost the performance since the MS-SSIM surpasses SSIM by almost 0.12 in terms of SRCC, which also confirms the rationality of the proposed hierarchical ST-t structure; (d) The poor performance of LPIPS can be explained that the LPIPS model is trained with images that have a huge gap with DHH projections, thus resulting in relatively unsatisfactory generalization performance on the proposed DHHQA database.

6. CONCLUSION

In this paper, we propose a large-scale digital human head quality assessment database to deal with the issues of digital human quality assessment. 55 reference DHHs are selected from the 254 human subjects and each reference DHH is degraded with 7 types of common distortions under 4 levels, which generates a total of 1,540 distorted DHH models. Then a subjective experiment is carried out to obtain the MOSs for the distorted DHH models in a well-controlled laboratory environment. Afterwards, a simple yet effective FR projection-based method is proposed by employing pretrained Swin Transformer tiny as the backbone. The hierarchical quality-aware features are extracted from the reference and distorted DHHs' front projections and fused with the multi-head attention module. The experimental results show that the proposed method outperforms the mainstream FR-IQA methods, which demonstrates its effectiveness for predicting the visual quality levels of DHHs.

7. REFERENCES

[1] Nadia Magnenat-Thalmann and Daniel Thalmann, “Virtual humans: thirty years of research, what next?,” *Springer The Visual Computer*, vol. 21, no. 12, pp. 997–1015, 2005.

[2] Wenmin Zhu, Xumin Fan, and Yanxin Zhang, “Applications and research trends of digital human models in the manufacturing industry,” *Elsevier VRH*, vol. 1, no. 6, pp. 558–579, 2019.

[3] Qi Yang, Hao Chen, Zhan Ma, Yiling Xu, Rongjun Tang, and Jun Sun, “Predicting the perceptual quality of point cloud: A 3d-to-2d projection-based exploration,” *IEEE TMM*, pp. 1–1, 2020.

[4] Qi Liu, Honglei Su, Zhengfang Duanmu, Wentao Liu, and Zhou Wang, “Perceptual quality assessment of colored 3d point clouds,” *IEEE TVCG*, 2022.

[5] Yipeng Liu, Qi Yang, Yiling Xu, and Le Yang, “Point cloud quality assessment: Dataset construction and learning-based no-reference metric,” *ACM TOMM*, 2022.

[6] Y. Nehmé, F. Dupont, J. P. Farrugia, P. Le Callet, and G. Lavoué, “Visual quality of 3d meshes with diffuse colors in virtual reality: Subjective and objective evaluation,” *IEEE TVCG*, vol. 27, no. 3, pp. 2202–2219, 2021.

[7] Yana Nehmé, Florent Dupont, Jean-Philippe Farrugia, Patrick Le Callet, and Guillaume Lavoué, “Textured mesh quality assessment: Large-scale dataset and deep learning-based quality metric,” *arXiv preprint arXiv:2202.02397*, 2022.

[8] Jun Liu, Amir Shahroudy, Mauricio Perez, Gang Wang, Ling-Yu Duan, and Alex C Kot, “Ntu rgb+ d 120: A large-scale benchmark for 3d human activity understanding,” *IEEE TPAMI*, vol. 42, no. 10, pp. 2684–2701, 2019.

[9] Amir Shahroudy, Jun Liu, Tian-Tsong Ng, and Gang Wang, “Ntu rgb+ d: A large scale dataset for 3d human activity analysis,” in *IEEE/CVF CVPR*, 2016, pp. 1010–1019.

[10] Julieta Martinez, Rayat Hossain, Javier Romero, and James J Little, “A simple yet effective baseline for 3d human pose estimation,” in *IEEE ICCV*, 2017, pp. 2640–2649.

[11] Dario Pavllo, Christoph Feichtenhofer, David Grangier, and Michael Auli, “3d human pose estimation in video with temporal convolutions and semi-supervised training,” in *IEEE/CVF CVPR*, 2019, pp. 7753–7762.

[12] Georgios Georgakis, Ren Li, Srikrishna Karanam, Terrence Chen, Jana Košecká, and Ziyan Wu, “Hierarchical kinematic human mesh recovery,” in *ECCV*. Springer, 2020, pp. 768–784.

[13] Matthew Loper, Naureen Mahmood, Javier Romero, Gerard Pons-Moll, and Michael J Black, “Smpl: A skinned multi-person linear model,” *ACM TOG*, vol. 34, no. 6, pp. 1–16, 2015.

[14] Zicheng Zhang, Wei Sun, Xiongkuo Min, Tao Wang, Wei Lu, and Guangtao Zhai, “No-reference quality assessment for 3d colored point cloud and mesh models,” *IEEE TCSVT*, 2022.

[15] Yu Fan, Zicheng Zhang, Wei Sun, Xiongkuo Min, Wei Lu, Tao Wang, Ning Liu, and Guangtao Zhai, “A no-reference quality assessment metric for point cloud based on captured video sequences,” *arXiv preprint arXiv:2206.05054*, 2022.

[16] “Bellus3d face scans,” Bellus3D, Inc, Oct 1, 2022 [Online], <https://www.bellus3d.com/>.

[17] Michael Garland and Paul S Heckbert, “Simplifying surfaces with color and texture using quadric error metrics,” in *IEEE Proceedings Visualization*, 1998, pp. 263–269.

[18] “Draco 3d data compression,” Google, Inc, Oct 1, 2022 [Online], <https://github.com/google/draco>.

[19] RECOMMENDATION ITU-R BT, “Methodology for the subjective assessment of the quality of television pictures,” *International Telecommunication Union*, 2002.

[20] Ze Liu, Yutong Lin, Yue Cao, Han Hu, Yixuan Wei, Zheng Zhang, Stephen Lin, and Baining Guo, “Swin transformer: Hierarchical vision transformer using shifted windows,” in *IEEE/CVF CVPR*, 2021, pp. 10012–10022.

[21] Jia Deng, Wei Dong, Richard Socher, Li-Jia Li, Kai Li, and Li Fei-Fei, “Imagenet: A large-scale hierarchical image database,” in *IEEE/CVF CVPR*, 2009, pp. 248–255.

[22] Diederik P Kingma and Jimmy Ba, “Adam: A method for stochastic optimization,” in *ICLR*, 2015.

[23] Zhou Wang, A.C. Bovik, H.R. Sheikh, and E.P. Simoncelli, “Image quality assessment: from error visibility to structural similarity,” *IEEE TIP*, vol. 13, no. 4, pp. 600–612, 2004.

[24] Z. Wang, E.P. Simoncelli, and A.C. Bovik, “Multiscale structural similarity for image quality assessment,” in *IEEE ACSSC*, 2003, vol. 2, pp. 1398–1402 Vol.2.

[25] Wufeng Xue, Lei Zhang, Xuanqin Mou, and Alan C. Bovik, “Gradient magnitude similarity deviation: A highly efficient perceptual image quality index,” *IEEE TIP*, vol. 23, no. 2, pp. 684–695, 2014.

[26] H.R. Sheikh and A.C. Bovik, “Image information and visual quality,” *IEEE TIP*, vol. 15, no. 2, pp. 430–444, 2006.

[27] Richard Zhang, Phillip Isola, Alexei A. Efros, Eli Shechtman, and Oliver Wang, “The unreasonable effectiveness of deep features as a perceptual metric,” in *IEEE/CVF CVPR*, 2018, pp. 586–595.